Accepted Manuscript

Synthesis and biological evaluation of 3-aryl-quinolin derivatives as anti-breast cancer agents targeting ERα and VEGFR-2

Xinyu Li, Chengzhe Wu, Xin Lin, Xuerong Cai, Linyi Liu, Guoshun Luo, Qidong You, Hua Xiang

PII: S0223-5234(18)30914-0

DOI: https://doi.org/10.1016/j.ejmech.2018.10.045

Reference: EJMECH 10831

To appear in: *European Journal of Medicinal Chemistry*

Received Date: 17 October 2017

Revised Date: 1 August 2018

Accepted Date: 18 October 2018

Please cite this article as: X. Li, C. Wu, X. Lin, X. Cai, L. Liu, G. Luo, Q. You, H. Xiang, Synthesis and biological evaluation of 3-aryl-quinolin derivatives as anti-breast cancer agents targeting ERα and VEGFR-2, *European Journal of Medicinal Chemistry* (2018), doi: https://doi.org/10.1016/j.ejmech.2018.10.045.

Graph abstract

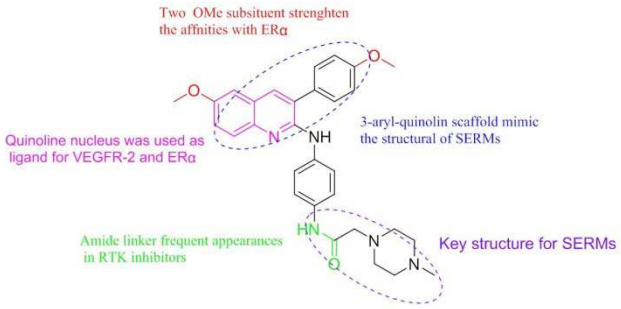

13f IC_{50}: 1.78 μM (ERα) 0.086 μM (VEGFR-2)
1.8 μM (MCF-7) 7.2 μM (HUVEC)
1.8 μM (Ishikawa)

Muti-targeted effects on ERα and VEGFR-2

Synthesis and biological evaluation of 3-aryl-quinolin derivatives as anti-breast cancer agents targeting ERα and VEGFR-2

Xinyu Li[a] , Chengzhe Wu[a], Xin Lin[a] , Xuerong Cai[a], Linyi Liu[a], Guoshun Luo[a], Qidong You[a], Hua Xiang[a,*]

[a]*Jiangsu Key Laboratory of Drug Design and Optimization, China Pharmaceutical University, 24 Tongjiaxiang, Nanjing 210009, PR China*

* Corresponding author. Tel.: +86 025 83271096; Fax: +86 025 83271096 (H. Xiang).

E-mail addresses: xianghua@cpu.edu.cn (H. Xiang)

Abstract

SERMs are a series of important small molecular compounds to modulate estrogen receptor, such as tamoxifen. Although these drugs have showed great benefits in the treatment of breast cancer, the risk of endometrial cancer and endocrine resistance restrict their use. The reasonable designing of multi-target drugs can decrease the side effects and improve the tolerance of antineoplastic agents Studies have identified that VEGFR-2 plays a pivotal role in tumor angiogenesis and drug resistance. Besides, a combination of Tamoxifen and low dose of a VEGFR-2 inhibitor was reported to maximize therapeutic efficacy as well as to retard SERM resistant tumor growth. In this work, a series of 3-aryl-quinolin derivatives were designed to target to ERα and VEGFR-2 to eliminate the disadvantages of SERMs. We identified that compounds **12f** and **13f** displayed highly ERα binding affinities as well as relative intensity VEGFR-2 inhibitory activities. Moreover, this two compounds exhibited excellent anti-proliferative activities against MCF-7 and HUVEC cell lines with low micromolar IC_{50} (1~8 μM). A further study confirmed that compound **13f** can reduce the expression of PgR mRNA, arrest cell cycle in MCF-7 breast cancer cells, and restrain the cell migration. Overall, based on the biological activities data, **13f** can be chosen as a potential anti-cancer lead compound for further studying.

Keywords: Estrogen receptor; VEGFR-2; Multi target; Anti-breast cancer.

1 Introduction

Breast cancer is the most frequent cancer among women worldwide, with an incidence that rises dramatically with age.[1] According to the clinicopathological determination of estrogen receptor, progesterone receptor, HER2, and Ki-67, BC can be divided into four subtypes, including :(a) Luminal A: ER and/or PgR positive, HER2 negative, Ki-67 low (<14 %). (b) Luminal B: ER and/or PgR positive, HER2 negative, Ki-67 high. (c) Erb-B2 overexpression: HER2, over-expressed, or amplified ER and PgR absent. (d) Basal-like :ER and PgR absent, HER2 negative.[2] Studies have found that nearly 70% of human diagnosed with breast cancer are ERα positive.[3] Obviously, it is meaningful to develop the effective drugs targeting to ERα for the treatment of breast cancer.

ERα, a subtype of ER, is a member of the large superfamily of nuclear receptors.[4] The continuous activation of ERα by estrogens could induce the proliferation of tumor cell. Thus, the blocking-up of ER signaling by competitively binding to ERα with anti-estrogens is an effective therapeutic strategy.[5] In fact, it has been a significant target in the pharmaceutical industry for many years.[6] Selective estrogen receptor modulators(SERMs) are a class of non-steroidal ER ligands which act as antagonists in breast tissue but agonist in other tissues such as cardiovascular system and bone.[7, 8] Tamoxifen, contain a triphenylethylene scaffold and a basic side chain, is the first generation SERM which is developed for the treatment of ER (+) breast cancer. It occupies the ligand-binding domain of ERα and blocks the dimerization of ERα with etrstrogen. Consequently, the conformational changes of ERα is prevented, which changes are essential for the activation of target gene of estrogen.[9] Since then, a series of compounds mimicking the structure of tamoxifen are reported for treatment of breast cancer [Figure1].[10]

Unfortunately, the clinical effectiveness of single target drugs is generally transitory, being followed by almost-inevitable resistance and relapses because of the adaptive nature and heterogeneity of tumor cells and tumor microenvironment.[11] Despite many women with breast cancer initially respond well to Tamoxifen, the side effects often emerge such as long-term treatment of Tamoxifen increases the occurrence of endometrial cancer, another common deficiency that limits the use of

SERMs is intrinsic and acquired drug resistance. [12, 13] Therefore, development of the novel ER ligand to minimize the side effects is urgently needed.

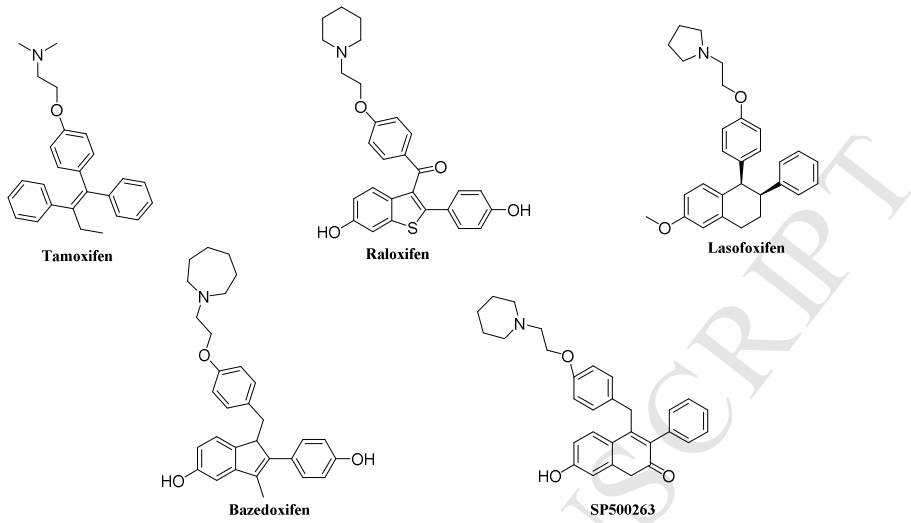

Figure 1. Previously reported selective estrogen receptor modulators (SERMs)

The drawbacks of single target drugs can be overcome by multiple target drugs which not only can increase therapeutic effectiveness and keep cancer cells from developing resistance therapeutic effects but also can avoid the risks involved in multicomponent drugs or drug cocktails, such as poor patient compliance, unpredictable pharmacokinetic/pharmacodynamics profiles and drug−drug interactions.[14, 15] Breast cancer is a hormone and angiogenesis dependent tumor whose growth, metastasis and invasion are related to tumor angiogenesis.[16] Vascular endothelial growth factor receptor-2, a member of the receptor tyrosine kinase family, has been proven to be the key mediator in tumor angiogenesis.[17] The Ras/Mitogen-activated protein kinase pathway which is activated in VEGF/VEGFR signal transduction plays an important role in promoting cell proliferation as well as tumor angiogenesis.[18, 19] Moreover, it is closely associated with Tamoxifen resistance.[20] Studies have revealed that the MAPK pathway can phosphorylate and activate ERα in a ligand-independent manner, resulting in transcription of estrogen-regulated genes and cell proliferation.[21] Research shows that VEGFR-2 inhibitors used as monotherapy are not sufficient in treating breast cancer.[22, 23] However, a combination of tamoxifen with a low dose of a VEGFR-2 inhibitor (Brivanib alaninate), was reported to maximize therapeutic efficacy as well as to retard SERM resistant tumor growth.[24]

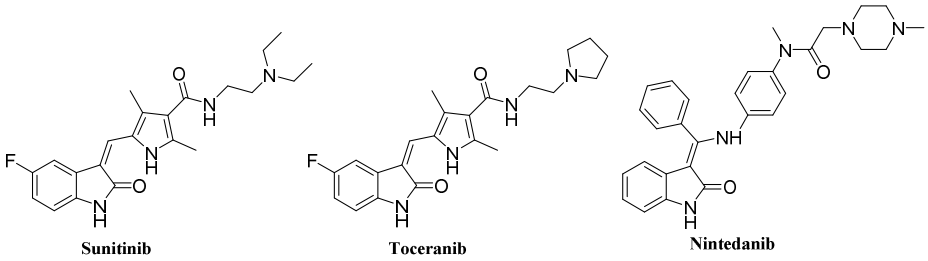

Figure 2. Previously reported VEGFR-2 inhibitors

Inspired by the above facts, VEGFR-2 inhibitors can both inhibit angiogenesis and retard SERMs resistance in breast cancer through the regulation of Ras/MAPK pathway. We have an assumption that weather a compound simultaneously targeting to ERα and VEGFR-2 can display a better effect for the treatment of breast cancer. By reviewing of literatures, we found that VEGFR-2 inhibitors such as Sunitinib containing an aromatic scaffold and flexible side chain with tertiary amine substituent at the end, which bears structural similarities with SERMs [Figure2]. Furthermore, a series of 2, 3-diaryl-isoquinolinone derivatives and 6-aryl-indenoisoquinolone derivatives as multiple ligands of ERα and VEGFR-2 previously reported by our group also proved our hypothesis [Figure 3].[25, 26]

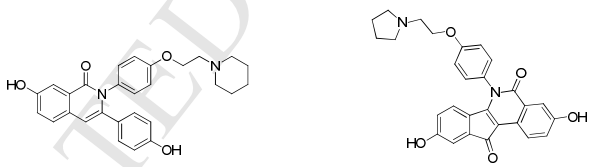

12
2, 3-diaryl isoquinolinone
dual ER-VEGFR-2 agent
ERα Inh% (0.1mg/ml) = 87.14%
VEGFR-2 Inh% (0.1mg/ml) = 84.83%

13
6-aryl-indenoisoquinolone
dual ER-VEGFR-2 agent
ERα IC_{50} = 7.2 μM
VEGFR-2 IC_{50} = 0.099 μM

Figure 3. Multiple ligands of ERα and VEGFR-2 together with outstanding biological results reported by our group previously

Recently, a series of VEGFR-2 inhibitors with the structure of quinoline drew our attention [Figure 4]. These compounds displayed similar structure that they all possess two oxygen substituents (most are methoxyl) and flexibility long-chain at C-6, 7 and C-4 of quinoline nucleus respectively. In addition, quinoline have been proven to be an excellent ERα ligand.[27] Based on these findings, we designed a series of 3-aryl-quinolin derivatives with various basic side chain at the end. The scaffold of 3-aryl-quinolin was expected to mimic the structural of SERMs. Amide side chains having the same

length of that in SERMs were used due to the frequent appearances in RTK inhibitors. Amides, arising commonly on the VEGFR-2 inhibitor were used to link the side chain to increase the inhibition of VEGFR-2. Methoxyl at C-7 or C-6 were used to mimic the estradiol to strengthen the affinity with ERα [Figure 5]. The biological activity and synthesis of designed compounds above are described in this paper.

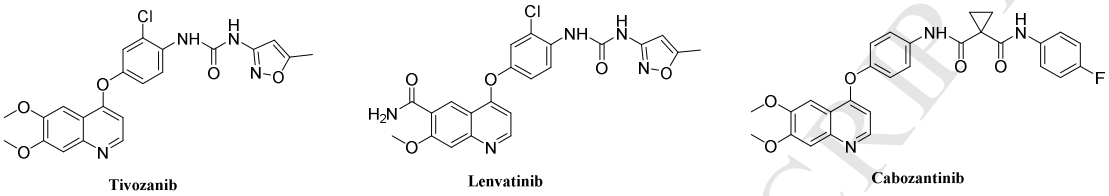

Figure 4. Selective VEGFR-2 inhibitors with quinolin or quinazoline structure

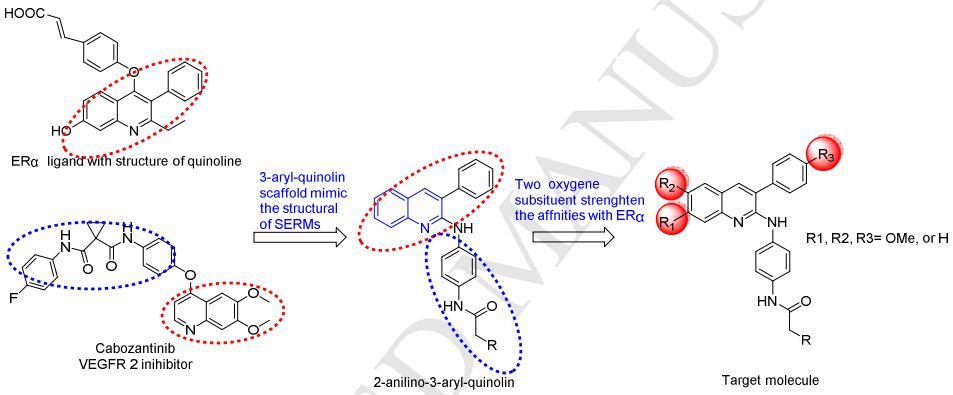

Figure 5. The rationally design of target compounds based on 2-anmilno-3-aryl-quinolin scaffold

2 Chemistry

The synthetic route of 3-aryl-quinolin derivative is described in Scheme 1. Amide **4** was obtained from 4-methoxyphenyl-acetic acid **2** by reaction with EDCI and 3-methoxyaniline **1**, then afforded quinolin nucleus **6** via Vilsmeier–Haack reaction. C-N coupling reaction between quinolin **6** and p-phenylenediamine provided the intermediate **8**, which converted to **10** using chloroacetyl chloride as raw materials and triethylamine as acid-binding agent. Finally, treatment **10** with various alkyl chlorides to provide target compounds **12a-f** in the presence of K_2CO_3.

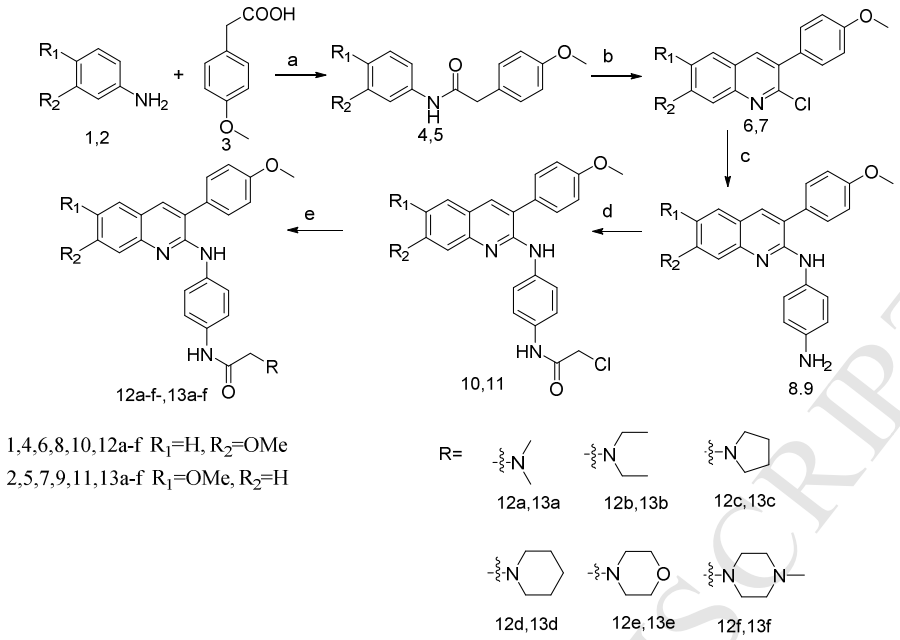

Scheme 1. Reagents and conditions: a. EDCI, HOBT, Et_3N, dichloromethane, rt, 10 h, 95-96%; b. DMF, $POCl_3$, 0 ℃-100 ℃, 4h, 62-65%; c. Cs_2CO_3, $Pd(OAc)_2$, BINAP, dioxane, reflux, 16 h, 62%; d. $ClCOCH_2Cl$, Et_3N, dichloromethane, 0℃, 0.5 h, 97-98%; e. DMF, K_2CO_3, KI, rt, 5 h, 64-87%.

3 Biological evaluation

3.1 ERα binding affinity and VEGFR-2 kinase inhibition assay

The ERα binding affinities of test compounds were determined by a fluorescence polarizationvet displacement assay using commercial estrogen receptor competitor assay with tamoxifen as positive control. As shown in [Table 1], most designed compounds displayed good activity with the ERα binding affinity more than 50% at the concentration of 20 μM. Different amino substituents made a difference in the activity. It was seemed that small size group more preferable in the side chain which showed better ERα binding affinity more than the bulkier group (**12a-c**, **13a-c vs. 12d-e**, **13d-e**). However, the excellent affinity was observed with compound **12f** and **13f** which possessed piperazine, a bulkier group, at the end. We speculated that the N-methyl might contribute to the activity due to a special interaction with the ERα. Furthermore, methoxy substituents at the C-6 or C-7 were also investigated. Obviously, compounds **12a-e** with methoxy at C-7 were more preferential than **13a-e.** But, interestingly, **13f** with a methoxy at C-6 presented the highest affinity (89.1%) which was greater than **12f** (82.1%). To confirm the result, we further measured the half-maximal inhibitory concentration (IC_{50}) of the potential compounds **12f**, **13f** with Tamoxifen as positive control. The IC_{50} of **13f** valued

at 1.78 μM, which is not only better than **12f** (IC_{50} = 2.33 μM) but also close to the tamoxifen (IC_{50} = 1.56 μM).

Once the binding affinity of our compounds with ERα was confirmed, we conducted the VEGFR-2 kinase inhibition assay by HTRF to verify the multi-target action [Table 1]. All designed compounds manifested inhibition on VEGFR-2 with Sunitinib as positive control. In general, methoxy at C-7 were more preferential than that at C-6 (**12a, 12b, 12f, 12d vs.13a, 13b, 13f, 13d**). In addition, significant effects can be found in inhibition for VEGFR-2 due to the different amino chains at the end. Four compounds **12-13d**, **13b**, **13f** displayed excellent activity IC_{50} < 100 nM, which possessed piperidine, diethylamine and methylpiperazine at the end respectively. Especially 12d, 13d with piperidine as amino side chain were regarded as most potential compounds which held inhibition value of 79 nM, 80nM respectively.

In summary, we can see that synthesized compounds exhibited from moderate to strong inhibitory activities compared with tamoxifen and sunitinib. Replaced the OMe at C-7 position of quinoline framework with OMe at C-6, most of the title compounds slightly decreased ERα binding affinity. However, it is in contrast to the inhibition for VEGFR-2, which showed that the OMe at C-7 is more preferable. Besides, the different groups introduced on terminal aniline have a large impact on both the ERα binding affinity and inhibition for VEGFR-2. The preliminary structure–activity relationship results were summarized in [Figure 7].

Table 1. The ERα binding affinities and VEGFR-2 kinase inhibition assay of test compounds.

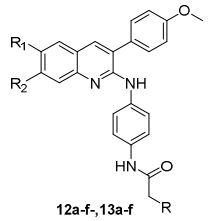

12a-f-,13a-f

Compound	R_1	R_2	R	ERα[a] Inh%(20 μM)	VEGFR-2[c] IC_{50}（nM）
12a	H	OMe		68.9	114
12b	H	OMe		72.1	101
12c	H	OMe		74.6	125
12d	H	OMe		45.1	79
12e	H	OMe		22.6	110
12f	H	OMe	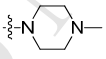	82.1	104
13a	OMe	H		45.3	109
.13b	OMe	H		63.8	81
13c	OMe	H		72.2	131
13d	OMe	H		52.4	80
13e	OMe	H		12.1	117
13f	OMe	H	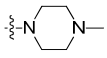	89.1	86
Tamoxifen				87.4	-
Sunitinib				-	65

[a]Percent inhibition of each compound was calculated from the polarization values.

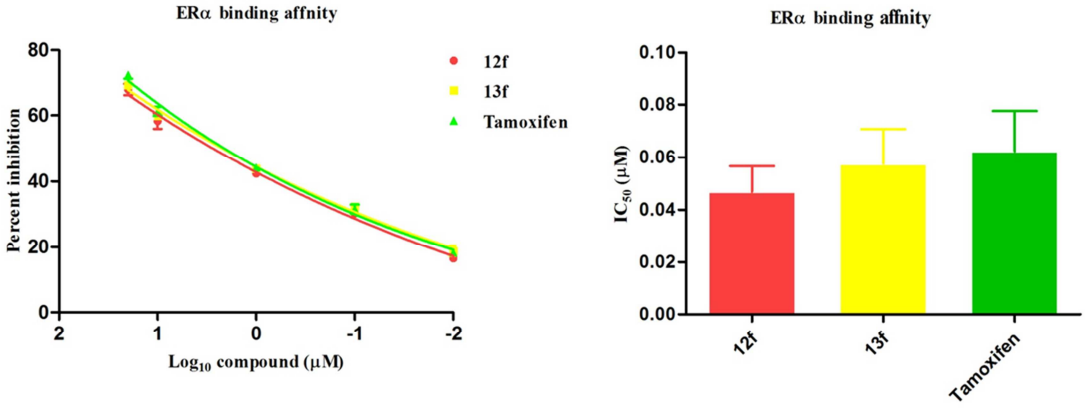

Figure 6. The half-maximal inhibitory concentration of selected compounds **12f**, **13f** and tamoxifen

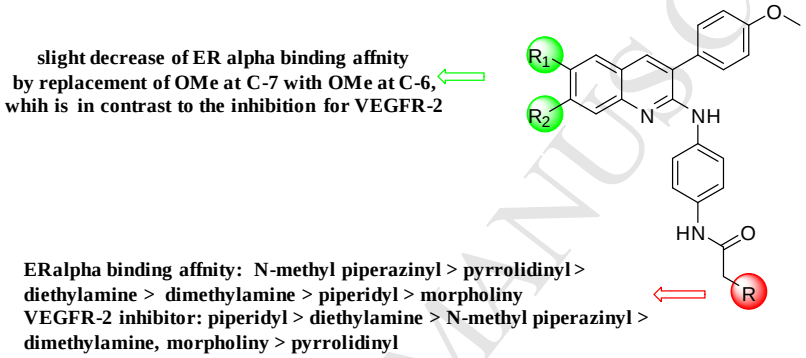

Figure 7. SARs of amino substituted 2-anmilno-3-aryl-quinolin **12a–f**, **13a–f.**

3.2 Cell anti-proliferative assay

HUVEC were used to evaluate the activity of VEGFR-2 inhibitors due to the activation of VEGFR-2 could promote its proliferation[28-30]. In addition, the assessment of anti-cancer activity was carried out through MCF-7 human breast cancer cells. As shown in [Table 2], most of the synthesized compounds exhibited comparative activities with positive control sunitinib, tamoxifen and raloxifen. Amusingly, compared with compounds **13a-e, 12a-e** with OMe at C-7 displayed better anti-proliferation both on HUVEC and MCF-7, which is irreconcilable with inhibition of VEGFR-2. Especially, **13d, 13e** with piperidine and morpholine at the end respectively held inhibition more than 50μM.We thought that the poor physicochemical property might be the main reason for their low anti-proliferation activity. Fortunately, there are four compounds (**12a**, **12c**, **12f**, **13f)** were found to exhibited the strong inhibitory effect against HUVEC cells MCF-7 cells (IC_{50} < 10 μM). It is worthy to note that the **12f**, **13f** with methylpiperazine as the side chain showed excellent cytotoxicity for MCF-7

(IC_{50} =2.8 μM and 1.8 μM respectively), which is better than reference compounds tamoxifen and raloxifen (IC_{50} =16.7 μM and 12.5 μM respectively). Maybe, the multi-target action contributed to their excellent activity, though their binding affinity of ERα are weaker than tamoxifen. Not only that, their potent anti-proliferative activities on HUVEC were comparable with the reference drug sunitinib (IC_{50} = 7.4 μM, 7.4 μM and 3.2 μM respectively).

Long-term using tamoxifen to treat ER+ breast cancer will lead to endometrial hyperplasia, making it more possibility for endometrial cancer. Therefore, anti-proliferative assay for Ishikawa was executed to estimate the effect of designed compounds for endometrium, accompanied with tamoxifen and raloxiefen as positive control. Some of these compounds reflected similar impact with tamoxifen and raloxifen that they show a proliferative effect on Ishikawa at low concentration of 10 μM or 1μM(data not show), but a anti-proliferative effect when the concentration beyond the 40μM. However, **12f** and **13f** still inhibited the growth of Ishikawa at this concentration with IC_{50} 3.8 μM, 1.8 μM respectively.

In summary, we found that compound **13f** displayed the strongest ERα binding affinity (IC_{50} = 1.78 μM) and excellent cytotoxicity for MCF-7 and Ishikawa cells (IC_{50} = 1.8 μM, both), also was a promising antiangiogenesis agent (86 nM of VEGFR-2 inhibition; IC_{50} = 7.4 μM against HUVEC cells). Thus, **13f** was selected for our further investigation of its multifunctional effects.

Table 2. Cell anti-proliferative assay with HUVEC，MCF-7 and Ishikawa.

Compound	HUVEC[a] IC_{50}(μM)	MCF-7[a] IC_{50}(μM)	Ishikawa[a] IC_{50}(μM)
12a	9.2	9.6	8.4
12b	14.0	17.3	21.4
12c	8.6	6.6	8.2
12d	23.5	47.9	>50
12e	9.1	>50	>50
12f	7.4	2.8	3.8
13a	22.2	39.5	>50
13b	45.6	>50	>50
13c	13.1	7.29	10.3
13d	>50	>50	>50
13e	>50	>50	>50
13f	7.4	1.8	1.8
Tamoxifen	ND[b]	16.7	>50
Raloxifen	ND[b]	12.5	>50
Sunitinib	3.2	-	14.3

[a]The concentration of compound that inhibit 50% of the cell growth after 48 h of drug exposure measured by MTT assay.

[b]Not determined

3.3 The inhibition activity of compound 13f against the expression of progestrone receptor microRNA in MCF-7 cells

Real-time polymerase chain reaction (RT-PCR) was performed in the ER positive MCF-7 cells to evaluate the modulation of progesterone receptor (PgR) [Figure 8]. Concentration at 10nM of estradiol(E2) was capable of elevating the mRNA expression of PgR gene compared with blank control. There was no significant effect on the mRNA expression level of PgR when used the 1 μM **13f** or Tamoxifen alone. However, **13f** at the concentration of 1 μM in combination with 10 nM E2 could reduce the expression of PgR mRNA and showed similar action compared to positive control tamoxifen, which indicated **13f** presented significantly anti-estrogenic property.

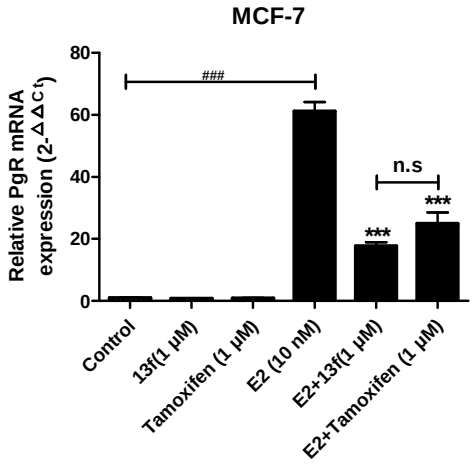

Figure 8. The increased mRNA expression of PR induced by E2 was reversed by **13f** in MCF-7 cells. The mRNA expression of PR was examined by Real-time PCR. Values are mean ±SD (n=3).* P < 0.05, ** P < 0.01, *** P < 0.001 vs. E2 group. # P< 0.05, ## P< 0.01, ### P< 0.001.

3.4 Effect of 13f on Cell Cycle distribution in human breast cancer MCF-7 cells

Many cytotoxic compounds exerted their anti-proliferative influence by either arresting the cell cycle at a particular check point of cell cycle or induction of apoptosis, or by a combined effect.[30] Regulation of the cell cycle and apoptosis are considered to be effective cancer therapeutic methods. The effect of **13f** on cell-cycle arrest of MCF-7 was assessed by flow cytometry assay. As shown in [Figure 9], Compared to untreated group, MCF-7 cells treated with **13f** for 12 h and 24 h increased 4.93% and 8.4% respectively in G1phase, which indicated that **13f** could arrest cell cycle at G1 phase.

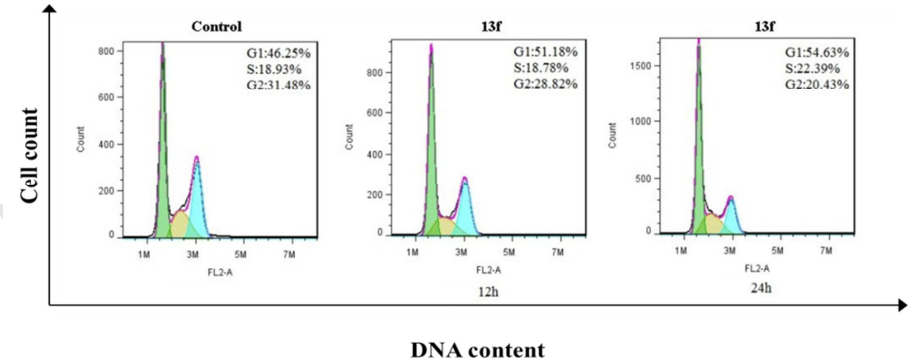

Figure 9. Cell cycle analysis of MCF-7 cells treatment of compound **13f** (1.25 μM) and DMSO as negative control for 12 h, 24 h.

3.5 Effect of 13f on migration of MCF-7 cells

Breast cancer metastasis plays a important role for the majority of deaths from breast cancer.[31] There is a significantly improvement on the survival of patients through the treatment for metastatic breast cancer.[32] Unfortunate, metastatic breast cancer is still considered as an incurable disease.[33, 34] Herein, the ability of **13f** to inhibit the migration of MCF-7 cells was determined by a wound-healing migration assay. The results obviously showed that in the absence of **13f**, the cells migrated to fill most of scratched area within 48 h, but the noncytotoxic treatment of **13f** significantly prevented this migration of MCF-7 cells in time-dependent manner [Figure 10], which was similarity to the positive control Sunitinib.

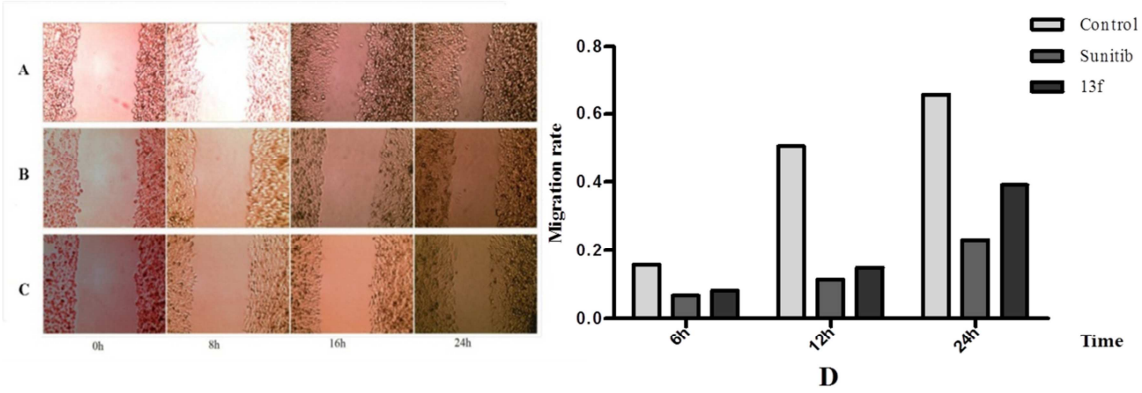

Figure 10. Effects on the migration of MCF-7. (A)Representative images of MCF-7 cells only treated with serum-free 1640 medium as negative control for 8 h, 16 h, and 48 h were photographed under phase contrast microscopy (magnification, 100×). (B)Positive control was treated with serum-free 1640 medium containing Sunitinib (1.25μM). (C)Test compound was treated with serum-free 1640 medium containing 13f (1.25 μM).（D）Migration rate of test compound.

4 Conclusion

We have designed and synthesized a series of 3-aryl-quinolin derivatives targeting both ERα and VEGFR-2, which is confirmed by biological evaluation of ERα binding affinities and VEGFR inhibition. These compounds were supposed to perform more effective anti-ERα positive breast cancer effects through inhibition of ERα and VEGFR-2 simultaneously. Further investigation also shows that

2-methylpiperazine at the end of side chains contribute most to the anti-proliferation effects against MCF-7 breast cancer cells and potential anti-angiogenesis effects in vitro. In addition, **12f, 13f** potentially eliminate the side effect for endometrium. Among all of our designed compounds, the mechanism of most potential compound **13f** were explored, which indicates that **13f** can reduce the E2-induced expression of PgR mRNA ,arrest cell cycle in MCF-7 breast cancer cells ,and restrain the cell migration. Above these facts show that **13f** could serve as promising lead candidates for further study.

5 Experimental section

5.1 Chemistry

5.1.1 General

Most chemicals and solvents were of analytical grade and, when necessary, were purified and dried by standard methods. Reactions were monitored by thin-layer chromatography (TLC) using precoated silica gel plates (silica gel GF/UV 254), and spots were visualized under UV light (254 nm). Melting points (uncorrected) were determined on a Mel-TEMP II melting point apparatus and are uncorrected. 1HNMR and 13CNMR spectra were recorded with a Bruker Avance 300 MHz spectrometer at 300 K, using TMS as an internal standard. MS spectra were recorded on a Shimadzu GC-MS 2050 (ESI) or an Agilent 1946A-MSD (ESI) Mass Spectrum. Column chromatography was performed with silica gel (200-300 mesh). Chemical shifts (d) are expressed in parts per million relative to tetramethylsilane, which was used as an internal standard, coupling constants (J) are in hertz (Hz), and the signals are designated as follows: s, singlet; d, doublet; t, triplet; m, multiplet.

*5.1.2 Synthesis of N-(3-methoxyphenyl)-2-(4-methoxyphenyl)acetamide (**4**)*

Compound **3** (5 g, 30.1 mmol), EDCI (5.78g, 30. 1 mmol), HOBt (4.06 g, 30.1 mmol) were dissolved in 100 mL CH_2Cl_2, and stirred for 1 h at 0 ℃. 4-methoxyaniline (3.7 g, 30.1 mmol) was then added into the mixture and stirred for 10 h at room temperature. The mixture was washed with saturated sodium chloride solution. The organic layer was evaporated under reduced pressure to give compound **4** as white solid (7.8 g, 96%).1H NMR (300 MHz, DMSO) δ:10.11 (s, 1H, NHCO), 7.37 – 7.29 (m, 1H, ArH), 7.28 – 7.07 (m, 4H, ArH), 6.93 – 6.83 (m, 2H, ArH), 6.66 – 6.56 (m, 1H, ArH),

3.72 (dd, 6H, OCH_3), 3.56 (s, CH_2CO). ^{13}C NMR (DMSO) δ 169.97, 159.94, 158.48, 140.92, 130.55, 129.93, 128.29, 114.17, 111.78, 109.07, 105.25, 55.46, 55.36, 42.97. MS (ESI, m/z):272.1 $[M+H]^+$.

*5.1.3 Synthesis of N,2-bis(4-methoxyphenyl)acetamide (**5**)*

Compound 5 was synthesized from compound 3 and 3-methoxyaniline using a procedure similar to that described for **4** as white solid (7.7 g, 95%). 1H NMR (300 MHz, Chloroform) δ 7.62 (s, 1H, NHCO), 7.29 – 7.08 (m, 4H, ArH), 6.97 – 6.86 (m, 3H, ArH), 6.72 – 6.52 (m, 1H, ArH), 3.81 (s, 3H, OCH_3), 3.75 (s, 3H, OCH_3), 3.63 (s, 2H, CH_2CO). ^{13}C NMR (75 MHz, DMSO-d_6) δ: 169.36, 158.43, 155.55, 132.88, 130.49, 128.52, 121.04, 114.25, 114.15, 55.58, 55.47, 42.79. MS (ESI, m/z):272.1 $[M+H]^+$.

*5.1.4 Synthesis of 2-chloro-7-methoxy-3-(4-methoxyphenyl)quinolone (**6**)*

DMF(3 mL, 38.7 mmol) was dropped into $POCl_3$ (12 mL, 129 mmol) at 0℃ and then stirred for 30 minutes. After that, compound 5 (7 g, 25.8 mmol) dissolved in 35ml DMF was added into the mixture and heated to 100℃ for 4 h. The reaction mixture was poured into water and was further extracted with ethyl acetate. The organic extracts were combined, dried over Na_2SO_4, filtered, and evaporated under vacuum and was subjected to column purification to furnish the desiredcompound **6** as yellow solid (5 g, 65%); ^1H NMR (300 MHz, Chloroform) δ: 7.92 (s, 1H, ArH), 7.62 (d, 1H, ArH), 7.41 – 7.33 (m, 2H, ArH), 7.30 (d, 1H, ArH), 7.14 (dd, 1H, ArH), 6.96 – 6.88 (m, 2H, ArH), 3.88 (s, 3H, OCH_3), 3.80 (s, 3H,OCH_3). ^{13}C NMR (Chloroform) δ 160.88, 158.99, 149.59, 148.00, 137.83, 131.51, 130.40, 129.65, 127.90, 122.00, 119.88, 113.19, 105.96, 55.12, 54.85. MS (ESI, m/z):300.1 $[M+H]^+$.

*5.1.5 Synthesis of 2-chloro-6-methoxy-3-(4-methoxyphenyl)quinolone (**7**)*

Compound **7** was synthesized from compound **5** using a procedure similar to that described for **6** as yellow solid (4.76 g, 62%); 1H NMR (300 MHz, Chloroform) δ 7.92 (d, 2H, ArH), 7.48 – 7.39 (m, 2H, ArH), 7.34 (dd, 1H, ArH), 7.06 – 6.95 (m, 3H, ArH), 3.89 (s, 3H, OCH_3), 3.85 (s, 3H,OCH_3). ^{13}C NMR (Chloroform) δ: 159.13, 157.78, 146.70, 142.22, 136.95, 134.10, 130.37, 129.58, 129.16, 127.91, 122.36, 113.20, 104.42, 55.10, 54.84. MS (ESI, m/z):300.1 $[M+H]^+$.

*5.1.6 Synthesis of N1-(7-methoxy-3-(4-methoxyphenyl)quinolin-2-yl)benzene-1,4-diamine (**8**)*

To a solution mixture of compound **6** (5 g, 16.7 mmol), p-phenylenediamine (2.7 g.25 mmol) in 1,4-dioxane (50 mL), the reagents of $Pd(OAc)_2$ (0.19 g,0.83 mmol), BINAP (1 g,1.67 mmol) and Cs_2CO_3(8.1 g, 25 mmol) were added. The mixture was heated to reflux under nitrogen atmosphere for 10h and then filtration, the filtrate was concentrated in vacuum. The rude product was purified by column chromatography to give compound **8** as yellow liquid (3.8 g, 62%);^{1}H NMR (300 MHz, Chloroform) δ: 7.62 (s, 1H,ArH), 7.54 – 7.37 (m, 5H, ArH), 7.20 (d, 1H, ArH), 7.06 – 6.98 (m, 2H, ArH), 6.91 (dd, 1H, ArH), 6.70 – 6.63 (m, 2H, ArH), 6.61 (s, 1H, NH), 3.92 (s, 3H, OCH_3), 3.85 (s, 3H, OCH_3), 3.55 (s, 2H, NH_2). ^{13}C NMR (Chloroform) δ: 160.30, 159.02, 152.03, 148.16, 141.34, 135.78, 131.47, 130.07, 129.08, 127.68, 122.69, 121.11, 118.29, 115.08, 114.31, 114.25, 105.59, 54.93, 54.87. MS (ESI, m/z):373.2 $[M+H]^+$.

*5.1.7 Synthesis of N1-(6-methoxy-3-(4-methoxyphenyl)quinolin-2-yl)benzene-1,4-diamine (**9**)*

Compound **9** was synthesized from compound 7 using a procedure similar to that described for **8** as yellow liquid (3.9g, 64%); ^{1}H NMR (300 MHz, DMSO) δ 7.62 (s, 1H, ArH), 7.38 (dd, 3H, ArH, NH), 7.26 (d, 2H, ArH), 7.05 (dd, 2H, ArH), 7.00 – 6.92 (m, 3H, ArH), 6.42 (d, 2H, ArH), 4.65 (s, 2H, NH_2), 3.69 (d, 6H, OCH_3). ^{13}C NMR (DMSO) δ 159.59, 155.01, 151.36, 144.17, 142.18, 136.07, 130.73, 130.69, 129.71, 127.59, 126.40, 124.63, 122.40, 120.76, 115.12, 114.35, 107.07, 55.72, 55.63. MS (ESI, m/z):373.2 $[M+H]^+$.

*5.1.8 Synthesis of 2-chloro-N-(4-((7-methoxy-3-(4-methoxyphenyl)quinolin-2-yl)amino)phenyl) acetamide (**10**)*

Chloroacetyl chloride (0.7 mL, 8.9 mmol) was dropped into the mixture of compound **8** (3 g, 8.1 mmol) and triethylamine (1.68 mL, 12.1mmol) in 20 mL CH_2Cl_2 at 0℃. The mixture was stirred for 1h and then washed with saturated sodium chloride solution. The reaction liquid was evaporated under reduced pressure to give compound **10** as yellow solid.

*5.1.9 Synthesis of 2-chloro-N-(4-((6-methoxy-3-(4-methoxyphenyl)quinolin-2-yl)amino) phenyl) acetamide (**11**)*

Compound **11** was synthesized from compound **9** using a procedure similar to that described for **10** as yellow solid.

*5.1.10 General procedures of synthesis of **12a-12f***

A suspension of compound **15** (0.4 g, 0.89 mmol), K_2CO_3 (0.24 g, 1.78 mmol) and different aliphatic amine (0.89 mmol) in 5mL DMF was stirred for 8 h at room temperature. The reaction liquid was poured into water. The precipitated product was collected by filtration, and further purified by silica gel column chromatography to provide the compound **12a-12f**.

*5.1.11 2-(dimethylamino)-N-(4-((7-methoxy-3-(4-methoxyphenyl)quinolin-2-yl)amino)phenyl)acetamide (**12a**)*

yellow solid, yield 86%; mp: 65-67℃; 1H-NMR (300MHz, CDCl3) δ: 9.06 (s, 1H, NHCO),6.78-7.79 (m, 13H, Ar-H, NH), 3.96 (s, 3H, OCH3), 3.89 (s, 3H, OCH3), 3.08(s, 2H, COCH2), 2.39(s,6H, N(CH3)2).13C-NMR ($CDCl_3$) δ: 167.94, 160.42, 159.15, 151.46, 147.91, 136.26, 136.01, 131.74, 130.07, 128.82, 127.69, 122.80, 119.51, 119.41, 118.52, 114.86, 114.35, 105.62, 63.17, 54.97, 54.90, 45.54; HRMS (ESI) m/z calcd for C27H28N4O3 $[M+H]^+$ 457.2234, found 457.2233.

*5.1.12 2-(diethylamino)-N-(4-((7-methoxy-3-(4-methoxyphenyl)quinolin-2-yl)amino)phenyl)acetamide (**12b**)*

Yellow solid, yield 72%; mp: 61-63℃; 1H-NMR (300MHz,CDCl3) δ: 9.36 (s, 1H, NHCO), 6.77-7.76 (m, 13H, Ar-H, NH), 3.96 (s, 3H, OCH3), 3.91 (s, 3H, OCH3), 3.16(s, 2H, COCH2), 2.63 (q,J=6.9, 4H, N(CH2CH3)2), 1.09 (t, J=7.1, 6H, N(CH2CH3)2); 13C-NMR ($CDCl_3$) δ: 169.30, 160.42, 159.16, 151.48, 147.92, 136.19, 136.01, 131.78, 130.08, 128.86, 127.67, 122.79, 119.50, 119.38, 118.52, 114.88, 114.35, 105.62, 57.64, 54.97, 54.91, 48.39, 11.98; HRMS (ESI) m/z calcd for $C_{29}H_{32}N_4O_3$ [M+H]+ 485.2547, found 485.2546.

*5.1.13 N-(4-((7-methoxy-3-(4-methoxyphenyl)quinolin-2-yl)amino)phenyl)-2-(pyrrolidin-1-yl)acetamide (**12c**)*

Yellow solid, yield 70%; mp: 81-83℃; ^{1}H-NMR (300MHz, $CDCl_3$) δ: 9.07 (s, 1H, NHCO), 6.78-7.79 (m, 13H, Ar-H, NH), 3.96 (s, 3H, OCH_3), 3.91 (s, 3H, OCH_3), 3.29(s, 2H, $COCH_2$), 2.71 (brs, 4H, $N(\underline{CH_2}CH_2)_2$), 1.87 (brs, 4H, $N(CH_2\underline{CH_2})_2$); ^{13}C-NMR ($CDCl_3$) δ: 168.37, 160.42, 159.15, 151.47, 147.91, 136.24, 136.03, 131.77, 130.08, 128.83, 127.70, 122.80, 119.63, 119.43, 118.52, 114.88, 114.35, 105.60, 59.25, 54.98, 54.92, 54.12, 23.59; HRMS (ESI) m/z calcd for $C_{29}H_{30}N_4O_3$ $[M+H]^+$ 483.2391, found 483.2398.

5.1.14 N-(4-((7-methoxy-3-(4-methoxyphenyl)quinolin-2-yl)amino)phenyl)-2-(piperidin-1-yl)ac

etamide (12d)

Yellow solid, yield 72%; mp: 174-176℃; ^{1}H-NMR (300MHz, $CDCl_3$) δ: 9.23 (s, 1H, NHCO), 6.78-7.79 (m, 13H, Ar-H, NH), 3.96 (s, 3H, OCH_3), 3.91 (s, 3H, OCH_3), 3.08(s, 2H, $COCH_2$), 2.56 (brs, 4H, $N(\underline{CH_2}CH_2)_2CH_2$), 1.63 (brs, 4H, $N(CH_2\underline{CH_2})_2CH_2$), 1.50 (brs, 2H, $N(CH_2CH_2)_2\underline{CH_2}$);^{13}C-NMR ($CDCl_3$) δ: 168.16, 160.42, 159.15, 151.46, 147.91, 136.22, 136.03, 131.79, 130.08, 128.83, 127.70, 122.79, 119.46, 118.52, 114.89, 114.35, 105.60, 62.29, 54.98, 54.92, 54.44, 25.84, 23.17; HRMS (ESI) m/z calcd for $C_{30}H_{32}N_4O_3$ $[M+H]^+$ 497.2547, found 497.2552.

*5.1.15 N-(4-((7-methoxy-3-(4-methoxyphenyl)quinolin-2-yl)amino)phenyl)-2-morpholinoaceta mide(**12e**)*

Yellow soild, yield 70%. mp: 93-95℃; ^{1}H-NMR (300MHz, $CDCl_3$) δ: 9.01 (s, 1H, NHCO), 6.79-7.78 (m, 13H, Ar-H, NH), 3.96 (s, 3H, OCH_3), 3.90 (s, 3H, OCH_3), 3.79(t, 4H, $N(CH_2\underline{CH_2})_2O$), 3.15(s, 2H, $COCH_2$), 2.64 (t, 4H, $N(\underline{CH_2}CH_2)_2O$); ^{13}C-NMR ($CDCl_3$) δ: 167.09, 160.45, 159.17, 151.42, 147.88, 136.48, 136.07, 131.42, 130.07, 128.79, 127.72, 122.80, 119.56, 119.43, 118.55, 114.93, 114.36, 105.60, 66.57, 61.95, 54.97, 54.91, 54.78, 53.31; HRMS (ESI) m/z calcd for $C_{29}H_{30}N_4O_4$ $[M+H]^+$ 499.234, found 499.2342.

*5.1.16 N-(4-((7-methoxy-3-(4-methoxyphenyl)quinolin-2-yl)amino)phenyl)-2-(4-methylpiperazi n-1-yl)acetamide(**12f**)*

Yellow soild, yield 64%. mp: 81-84℃; ^{1}H-NMR (300MHz, $CDCl_3$) δ: 9.11 (s, 1H, NHCO), 6.78-7.79 (m, 13H, Ar-H, NH), 3.96 (s, 3H, OCH_3), 3.90 (s, 3H, OCH_3), 3.15(s, 2H, $COCH_2$), 2.68 (brs, 4H, $N(\underline{CH_2}CH_2)_2NCH_3$), 2.53 (brs, 4H, $N(CH_2\underline{CH_2})_2NCH_3$), 2.34 (s, 3H, $N(CH_2CH_2)_2N\underline{CH_3}$); ^{13}C-NMR ($CDCl_3$) δ: 167.48, 160.43, 159.16, 151.44, 147.89, 136.35, 136.05, 131.59, 130.08, 128.81, 127.70, 122.80, 119.48, 119.45, 118.54, 114.91, 114.36, 105.60, 61.35, 54.97, 54.91, 54.78, 52.92, 45.50; HRMS (ESI) m/z calcd for $C_{30}H_{33}N_5O_3$ $[M+H]^+$ 512.26, found 512.2654

*5.1.17 2-(dimethylamino)-N-(4-((6-methoxy-3-(4-methoxyphenyl)quinolin-2-yl)amino)phenyl)a cetamide(**13a**)*

Yellow soild, yield 84%. mp: 184-186℃; ^{1}H-NMR (300MHz, $CDCl_3$) δ: 9.05 (s, 1H, NHCO), 6.71-7.80 (m, 13H, Ar-H, NH), 3.91 (s, 3H, OCH_3), 3.90 (s, 3H, OCH_3), 3.09(s, 2H, $COCH_2$), 2.40(s,

6H, $N(CH_3)_2$); ^{13}C-NMR ($CDCl_3$) δ: 167.92, 159.28, 155.13, 149.65, 141.72, 136.57, 135.46, 131.42, 129.99, 128.75, 127.76, 125.65, 124.15, 120.35, 119.55, 118.87, 114.36, 105.57, 63.18, 55.03, 54.92, 45.56; HRMS (ESI) m/z calcd for $C_{27}H_{28}N_4O_3$ $[M+H]^+$ 457.2234, found 457.2232.

*5.1.18 2-(diethylamino)-N-(4-((6-methoxy-3-(4-methoxyphenyl)quinolin-2-yl)amino)phenyl)acetamide(**13b**)*

Yellow soild ,yield 87%. mp: 144-146℃; ^{1}H-NMR (300MHz, $CDCl_3$) δ: 9.35 (s, 1H, NHCO), 6.71-7.79 (m, 13H, Ar-H, NH), 3.89 (s, 3H, OCH_3), 3.88 (s, 3H, OCH_3), 3.15(s, 2H, $COCH_2$), 2.62 (q, J=7.1, 4H, $N(\underline{CH_2}CH_3)_2$), 1.08 (t, J=7.1, 6H, $N(CH_2\underline{CH_3})_2$); ^{13}C-NMR ($CDCl_3$) δ: 169.27, 159.27, 155.10, 149.63, 141.70, 136.51, 135.47, 131.47, 129.97, 128.72, 127.71, 125.63, 124.17, 120.61, 119.41, 118.93, 114.35, 105.56, 57.61, 55.01, 54.91, 48.38, 11.97; HRMS (ESI) m/z calcd for $C_{29}H_{32}N_4O_3$ $[M+H]^+$ 485.2547, found 485.2548.

*5.1.19 N-(4-((6-methoxy-3-(4-methoxyphenyl)quinolin-2-yl)amino)phenyl)-2-(pyrrolidin-1-yl)acetamide(**13c**)*

Yellow soild yield 86%. mp: 162-164℃; ^{1}H-NMR (300MHz, $CDCl_3$)δ: 9.04 (s, 1H, NHCO), 6.71-7.80 (m, 13H, Ar-H, NH), 3.91 (s, 3H, OCH_3), 3.90 (s, 3H, OCH_3), 3.29(s, 2H, $COCH_2$), 2.71 (brs, 4H, $N(\underline{CH_2}CH_2)_2$), 1.87 (brs, 4H, $N(CH_2\underline{CH_2})_2$); ^{13}C-NMR ($CDCl_3$) δ: 168.33, 159.29, 155.13, 149.66, 141.73, 136.57, 135.45, 131.48, 129.98, 128.75, 127.73, 125.65, 124.17, 120.36, 119.65, 118.89, 114.37, 105.60, 59.29, 55.03, 54.91, 54.12, 23.60; HRMS (ESI) m/z calcd for $C_{29}H_{30}N_4O_3$ $[M+H]^+$ 483.2391, found 483.2387.

*5.1.20 N-(4-((6-methoxy-3-(4-methoxyphenyl)quinolin-2-yl)amino)phenyl)-2-(piperidin-1-yl)acetamide(**13d**)*

Yellow soild ,yield 87%. mp: 170-173℃; ^{1}H-NMR (300MHz, $CDCl_3$) δ: 9.21 (s, 1H, NHCO), 6.72-7.79 (m, 13H, Ar-H, NH), 3.88 (s, 3H, OCH_3), 3.87 (s, 3H, OCH_3), 3.07(s, 2H, $COCH_2$), 2.54 (brs, 4H, $N(\underline{CH_2}CH_2)_2CH_2$), 1.62 (brs, 4H, $N(CH_2\underline{CH_2})_2CH_2$), 1.50 (brs, 2H, $N(CH_2CH_2)_2\underline{CH_2}$);^{13}C-NMR ($CDCl_3$) δ: 168.10, 159.27, 155.11, 149.63, 141.69, 136.53, 135.45, 131.47, 129.97, 128.72, 127.70, 125.63, 124.17, 120.35, 119.49, 118.90, 114.35, 105.57, 62.31, 55.01, 54.90, 54.43, 25.82, 23.18; HRMS (ESI) m/z calcd for $C_{30}H_{32}N_4O_3$ $[M+H]^+$ 497.2547, found 497.2537.

*5.1.21 N-(4-((6-methoxy-3-(4-methoxyphenyl)quinolin-2-yl)amino)phenyl)-2-morpholinoacetamide(**13e**)*

Yellow soild, yield 82%. mp: 185-186℃; ^{1}H-NMR (300MHz, $CDCl_3$) δ: 8.99 (s, 1H, NHCO), 6.72-7.79 (m, 13H, Ar-H, NH), 3.91 (s, 3H, OCH_3), 3.90 (s, 3H, OCH_3), 3.80(t, 4H, $N(CH_2\underline{CH_2})_2O$), 3.15(s, 2H, $COCH_2$), 2.64 (t, 4H, $N(\underline{CH_2}CH_2)_2O$);^{13}C-NMR ($CDCl_3$) δ: 167.06, 159.30, 155.17, 149.61, 141.68, 136.78, 135.50, 131.11, 129.98, 128.72, 127.72, 125.65, 124.19, 120.39, 119.61, 118.91, 114.37, 105.59, 66.57, 61.97, 55.03, 54.92, 53.32; HRMS (ESI) m/z calcd for $C_{29}H_{30}N_4O_4$ $[M+H]^+$ 499.234, found 499.2336.

*5.1.22 N-(4-((6-methoxy-3-(4-methoxyphenyl)quinolin-2-yl)amino)phenyl)-2-(4-methylpiperazin-1-yl)acetamide(**13f**)*

Yellow soild, 76%.mp: 177-179℃; ^{1}H-NMR (300MHz, $CDCl_3$) δ: 9.06 (s, 1H, NHCO), 6.71-7.79 (m, 13H, Ar-H, NH), 3.91 (s, 3H, OCH_3), 3.90 (s, 3H, OCH_3), 3.15(s, 2H, $COCH_2$), 2.68 (brs, 4H, $N(\underline{CH_2}CH_2)_2NCH_3$), 2.53 (brs, 4H, $N(CH_2\underline{CH_2})_2NCH_3$), 2.35 (s, 3H, $N(CH_2CH_2)_2N\underline{CH_3}$); ^{13}C-NMR ($CDCl_3$) δ: 167.44, 159.30, 155.15, 149.63, 141.70, 136.66, 135.48, 131.29, 129.98, 128.74, 127.72, 125.65, 124.18, 120.37, 119.53, 118.92, 114.35, 105.59, 61.37, 55.03, 54.92, 54.78, 52.94, 45.50; HRMS (ESI) m/z calcd for $C_{30}H_{33}N_5O_3$ $[M+H]^+$ 512.2656, found 512.2661.

5.2 Biological evaluation

5.2.1 ERα Binding Affinity Assay

The recombinant ERα (Thermo Fisher Scientific Inc., Invitrogen, USA) and the fluorescent estrogen ligands (self-made) were removed from the -80^{o}C freezer and thawed on ice for 1h prior to use. The fluorescent estrogen ligand was added to the ERα and screening buffer (ES2 Screening Buffer, Invitrogen, USA) was added to make the final concentration 9 nM for fluorescent estrogen and 30 nM for ERα. Test compounds were accurately weighed and dissolved in DMSO, screening buffer was added to dilute to required concentration. Test compound (1 μL) was added to 49 μL screening buffer in each well (384-well microplate, Corning, USA). To this 50 μL of the fluorescent estrogen/ER complex was added to make up a final volume of 100 μL. A positive control contained 50 μL estradiol buffer (1nM) and 50 μL fluorescent estrogen/ER complex. A negative control contained 50 μL screening

buffer and 50 μL fluorescent estrogen/ER complex. The negative control was used to determine the polarization value when no competitor was present (theoretical maximum polarization). The microplate was incubated in the dark at room temperature for 2 h and shaken on a plate shaker. The polarization values were read on a Safire microplate reader and used to calculate the IC_{50} values.

5.2.2 VEGFR-2 kinase inhibitory assay

VEGFR-2 kinase assay was conducted using homogeneous time resolved fluorescence (HTRF) assay. The general procedures were as following: VEGFR-2 kinase (Invitrogen, USA), substrates, ATP and test compounds were mixed and incubated in a final buffer with the total volume of 10 mL in 384-well microplate. Wells containing the substrate and the kinase without compound were used as total reaction control. The assay plate was incubated at room temperature in the dark for 1 h. Detection was performed with HTRF module of Beckman Coulter detection platform to get the fluorescence values which were further used to calculate the IC_{50} values.

5.2.3 MTT assay for anti-proliferative activities

Cells were cultured in RPMI1640 medium (containing 10% (v/v) FBS, 100 U/mL Penicillin and 100 mg/mL Streptomycin) in a 5% CO_2-humidified atmosphere at 37^{o}C. Cells were trypsinized and seeded at a density of 1 x 10^5/mL into a 96-well plate (100 mL/well) and incubated at 37^{o}C, 5% CO_2 atmosphere for 24 h. After this time they were treated with 100 mL/well medium containing test compounds which had been pre-prepared to provide the concentration range of and re-incubated for a further 48 h. Control wells were added the equivalent volume of medium containing 1% (v/v) DMSO. 20 μL MTT (5 mg/mL) was added and cells continued to incubate in darkness at 37^{o}C for 4 h. The culture medium was then removed carefully and 150 mL DMSO was added. The cells were maintained at room temperature in darkness for 20 min to ensure thorough color diffusion before reading the absorbance. The absorbance values were read at 490 nm for determination of IC_{50} values.

5.2.4 Real-Time Polymerase Chain Reaction (RT-PCR).

RNA samples were reverse transcribed to cDNA and the PCR reactions were performed using TaKaRa SYBR Green Master Mix (Code. no. 638320) carried out in StepOnePlus^{TM} Real-Time PCR instrument (4376600, Life Technologies). The program for amplification was 1 cycle of 95°C for 2 min

followed by 40 cycles of 95°C for 10 s, 60°C for 30 s, and 95°C for 10 s. The PCR results were normalized to GAPDH expression and were quantified by the ΔΔCT method.

5.2.5 Cell migration assay

Cell migration assay were carried out using 24-well plate and wound-healing method. Briefly, MCF-7 cells were seeded in a 24-well plate and were allowed to grow to 100% confluence. Cell culture were injured by a 10 mL tip, cells were washed twice with PBS, and then incubated with fresh medium with or without compound **13f** at 1.25μM for 8h, 16h and 24h. Cell migration to the damaged area was then visualized and photographed on a phase contrast microscope. The detailed value was calculated by Image J, and then it was analyzed through the GraphPad Prism 5.

5.2.6 Cell cycle analysis

The MCF-7 cells were treated with 1.25 μM of **13f** for 12h and 24 h. After treatment, the cells were washed twice with ice-cold PBS, collected by centrifugation, and fixed in ice-cold 70% (v/v) ethanol, washed with PBS, re-suspended with 0.1 mg/mL RNase, stained with 40 mg/mL PI, and analyzed by flow cytometry using FACScalibur (Becton Dickinson). The cell cycle distributions were calculated using Flowjo 7.6.1 software..

Supplementary data

Supplementary data (the ^{1}H NMR, ^{13}C NMR and HRMS spectra of target compounds associated with this article can be found, in the online version, at.

Acknowledgements

This work was supported by grants from the Natural Science Foundation of China (NSFC, 81373279) and the Twelfth Five-Year Plan Major Project of Candidate Drugs (Ministry of National Science and Technology, 2012ZX09103101048). The authors are grateful to *Nanjing Paopao Biotechnology Co., Ltd* for performing the Western Blot experiment.

Abbreviations

ER, estrogen receptor; SERMs, selective estrogen receptor modulators; VEGF, Vascular endothelial growth factor; VEGFR-2, Vascular endothelial growth factor receptor-2; RTK, receptor tyrosine kinase; MAPK, mitogen-activated protein kinase; ERK, extracellular regulated kinases; HUVEC, human

umbilical vein endothelial cell; RT-PCR, real-time polymerase chain reaction; PgR, progesterone receptor; E2, estradiol; BC, Breast cancer; HER2 human epidermal growth factor receptor-2; SARs, structure–activity relationships.

References and notes

[1] J. Ferlay, I. Soerjomataram, R. Dikshit, S. Eser, C. Mathers, M. Rebelo, D.M. Parkin, D. Forman, F. Bray, Cancer incidence and mortality worldwide: Sources, methods and major patterns in GLOBOCAN 2012, International Journal of Cancer, 136 (2015) E359-E386.

[2] A. Goldhirsch, W.C. Wood, A.S. Coates, R.D. Gelber, B. Thurlimann, H.J. Senn, m. Panel, Strategies for subtypes--dealing with the diversity of breast cancer: highlights of the St. Gallen International Expert Consensus on the Primary Therapy of Early Breast Cancer 2011, Ann Oncol, 22 (2011) 1736-1747.

[3] S. Sommer, S.A. Fuqua, Estrogen receptor and breast cancer, Seminars in Cancer Biology, 11 (2001) 339-352.

[4] X. Li, J. Huang, P. Yi, R.A. Bambara, R. Hilf, M. Muyan, Single-chain estrogen receptors (ERs) reveal that the ERalpha/beta heterodimer emulates functions of the ERalpha dimer in genomic estrogen signaling pathways, Molecular & Cellular Biology, 24 (2004) 7681.

[5] L. Liu, Z. Tang, C. Wu, X. Li, A. Huang, X. Lu, Q. You, H. Xiang, Synthesis and biological evaluation of 4,6-diaryl-2-pyrimidinamine derivatives as anti-breast cancer agents, Bioorganic & Medicinal Chemistry Letters, 28 (2017) 1138-1142.

[6] A. Lai, M. Kahraman, S. Govek, J. Nagasawa, C. Bonnefous, J. Julien, K. Douglas, J. Sensintaffar, N. Lu, K.J. Lee, Identification of GDC-0810 (ARN-810), an Orally Bioavailable Selective Estrogen Receptor Degrader (SERD) that Demonstrates Robust Activity in Tamoxifen-Resistant Breast Cancer Xenografts, Journal of Medicinal Chemistry, 58 (2015) 4888.

[7] K. Maruyama, M. Nakamura, S. Tomoshige, K. Sugita, M. Makishima, Y. Hashimoto, M. Ishikawa, Structure-activity relationships of bisphenol A analogs at estrogen receptors (ERs): discovery of an ERα-selective antagonist, Bioorganic & Medicinal Chemistry Letters, 23 (2013) 4031-4036.

[8] Z. Bai, R. Gust, Breast Cancer, Estrogen Receptor and Ligands, Archiv Der Pharmazie, 342 (2009) 133-149.

[9] M. Dutertre, C.L. Smith, Dutertre, M. & Smith, C.L. Molecular mechanisms of selective estrogen receptor modulator (SERM) action. J. Pharmacol. Exp. Ther. 295, 431-437, Journal of Pharmacology & Experimental Therapeutics, 295 (2000) 431-437.

[10] T. Wang, Q. You, F.S. Huang, H. Xiang, Recent advances in selective estrogen receptor modulators for breast cancer, Mini Reviews in Medicinal Chemistry, 9 (2009) -.

[11] J. Zang, X. Liang, Y. Huang, Y. Jia, X. Li, W. Xu, C.J. Chou, Y. Zhang, Discovery of Novel Pazopanib-based HDAC and VEGFR Dual Inhibitors Targeting Cancer Epigenetics and Angiogenesis Simultaneously, Journal of Medicinal Chemistry, (2018).

[12] F.E. van Leeuwen, J. Benraadt, J.W. Coebergh, L.A. Kiemeney, C.H. Gimbrère, R. Otter, L.J. Schouten, R.A. Damhuis, M. Bontenbal, F.W. Diepenhorst, Risk of endometrial cancer after tamoxifen treatment of breast cancer, Lancet, 343 (1994) 448.

[13] E.A. Musgrove, R.L. Sutherland, Biological determinants of endocrine resistance in breast cancer,

Nature Reviews Cancer, 9 (2009) 631.

[14] R. Morphy, Z. Rankovic, Designed multiple ligands. An emerging drug discovery paradigm, Journal of Medicinal Chemistry, 48 (2005) 6523-6543.

[15] N.M. O'Boyle, M.J. Meegan, Designed multiple ligands for cancer therapy, Current Medicinal Chemistry, 18 (2011) 4722-4737.

[16] D.J. Hicklin, L.M. Ellis, Role of the vascular endothelial growth factor pathway in tumor growth and angiogenesis, Journal of Clinical Oncology, 23 (2005) 1011-1027.

[17] J.D. Yan, Y. Liu, Z.Y. Zhang, G.Y. Liu, J.H. Xu, L.Y. Liu, Y.M. Hu, Expression and prognostic significance of VEGFR-2 in breast cancer, Pathology, research and practice, 211 (2015) 539.

[18] D. Huang, Y. Ding, W.M. Luo, S. Bender, C.N. Qian, E. Kort, Z.F. Zhang, K. Vandenbeldt, N.S. Duesbery, J.H. Resau, Inhibition of MAPK kinase signaling pathways suppressed renal cell carcinoma growth and angiogenesis in vivo, Cancer Research, 68 (2008) 81.

[19] G. Mavria, Y. Vercoulen, M. Yeo, H. Paterson, M. Karasarides, R. Marais, D. Bird, C.J. Marshall, ERK-MAPK signaling opposes Rho-kinase to promote endothelial cell survival and sprouting during angiogenesis, Cancer Cell, 9 (2006) 33-44.

[20] L.M. Mcglynn, T. Kirkegaard, J. Edwards, S. Tovey, D. Cameron, C. Twelves, J.M. Bartlett, T.G. Cooke, Ras/Raf-1/MAPK pathway mediates response to tamoxifen but not chemotherapy in breast cancer patients, Clinical Cancer Research An Official Journal of the American Association for Cancer Research, 15 (2009) 1487.

[21] P. Ascenzi, A. Bocedi, M. Marino, Structure-function relationship of estrogen receptor alpha and beta: impact on human health, Molecular Aspects of Medicine, 27 (2006) 299-402.

[22] M.E. Fratto, M. Imperatori, B. Vincenzi, F. Tomao, D. Santini, G. Tonini, New perspectives: role of Sunitinib in breast cancer, La Clinica Terapeutica, 162 (2011) 251-257.

[23] G. Ranieri, R. Patruno, E. Ruggieri, S. Montemurro, P. Valerio, D. Ribatti, Vascular endothelial growth factor (VEGF) as a target of bevacizumab in cancer: from the biology to the clinic, Current Medicinal Chemistry, 13 (2006) 1845-1857.

[24] R.R. Patel, S. Sengupta, H.R. Kim, A.J. Kleinszanto, J.R. Pyle, F. Zhu, T. Li, E.A. Ross, S. Oseni, J. Fargnoli, Experimental Treatment of Estrogen Receptor (ER) Positive Breast Cancer with Tamoxifen and Brivanib Alaninate, a VEGFR-2/FGFR-1 Kinase Inhibitor: a potential clinical application of angiogenesis inhibitors, European Journal of Cancer, 46 (2010) 1537.

[25] Z. Tang, S. Niu, F. Liu, K. Lao, J. Miao, J. Ji, X. Wang, M. Yan, L. Zhang, Q. You, Synthesis and biological evaluation of 2,3-diaryl isoquinolinone derivatives as anti-breast cancer agents targeting ERα and VEGFR-2, Bioorganic & Medicinal Chemistry Letters, 24 (2014) 2129-2133.

[26] Z. Tang, C. Wu, T. Wang, K. Lao, Y. Wang, L. Liu, M. Muyaba, P. Xu, C. He, G. Luo, Design, synthesis and evaluation of 6-aryl-indenoisoquinolone derivatives dual targeting ERα and VEGFR-2 as anti-breast cancer agents, European Journal of Medicinal Chemistry, 118 (2016) 328.

[27] W.J. Hoekstra, H.S. Patel, X.J. Liang, D.O. Heyer, T.M. Willson, M.A. Iannone, S.H. Kadwell, L.A. Miller, K.H. Pearce, C.A. Simmons, Discovery of novel quinoline-based estrogen receptor ligands using peptide interaction profiling, Journal of Medicinal Chemistry, 48 (2005) 2243-2247.

[28] S.M. Wilhelm, C. Carter, L. Tang, D. Wilkie, A. McNabola, H. Rong, C. Chen, X. Zhang, P. Vincent, M. McHugh, Y. Cao, J. Shujath, S. Gawlak, D. Eveleigh, B. Rowley, L. Liu, L. Adnane, M. Lynch, D. Auclair, I. Taylor, R. Gedrich, A. Voznesensky, B. Riedl, L.E. Post, G. Bollag, P.A. Trail, BAY 43-9006 exhibits broad spectrum oral antitumor activity and targets the RAF/MEK/ERK pathway and receptor tyrosine kinases involved in tumor progression and angiogenesis, Cancer Res, 64 (2004) 7099-7109.

[29] H. Gelderblom, J. Verweij, N. Steeghs, E.D. Koning, A.V. Erkel, L.V. Doorn, M. Zuehlsdorf, P. Rajagopalan, O. Christensen, F. Eskens, 72 POSTER Phase I, safety, pharmacokinetic and biomarker study of telatinib (BAY 57-9352), an oral VEGFR-2 inhibitor, in a continuous schedule in patients with advanced solid tumors, Ejc Supplements, 4 (2006) 26-26.

[30] K.T. Chan, F.Y. Meng, Q. Li, C.Y. Ho, T.S. Lam, Y. To, W.H. Lee, M. Li, K.H. Chu, M. Toh, Cucurbitacin B induces apoptosis and S phase cell cycle arrest in BEL-7402 human hepatocellular carcinoma cells and is effective via oral administration, Cancer Letters, 294 (2010) 118-124.

[31] A. Maiti, K. Takabe, N.C. Hait, Metastatic triple-negative breast cancer is dependent on SphKs/S1P signaling for growth and survival, Cellular Signalling, 32 (2017) 85-92.

[32] S.K. Chia, C.H. Speersc, M.D. Yulia D'yachkova, M.D. Anna Kang, S. Malfair-Taylor, J.B. Bsc, A. Coldman, K.A. Gelmon, S.E. O'Reilly, I.A. Olivotto, The impact of new chemotherapeutic and hormone agents on survival in a population‐based cohort of women with metastatic breast cancer, Breast Diseases, 110 (2007) 973–979.

[33] A. Nicolini, R. Giardino, A. Carpi, P. Ferrari, L. Anselmi, S. Colosimo, M. Conte, M. Fini, G. Giavaresi, P. Berti, Metastatic breast cancer: an updating, Biomedicine & Pharmacotherapy, 60 (2006) 548-556.

[34] T. Luu, C. Chung, G. Somlo, Combining Emerging Agents in Advanced Breast Cancer, Oncologist, 16 (2011) 760-771.

Highlights

- Twelve 3-aryl-quinolin derivatives were evaluated as dual ERα/VEGFR-2 ligands
- **13f** exhibited potent activities in both enzymatic and cellular assays
- **13f** induced apoptosis and inhibited migration on MCF-7 cells
- **13f** reduced the expression of PgR mRNA